Response to reviewer 3 (2^{nd} round)

Reviewer's comments are presented here by italics

Comments:
General
The revised version is significantly better than the submitted one. However, there are still many points that need to be improved and clarified. The discussion and interpretation of the results is based on measured range-corrected signals (attenuated backscatter) and volume depolarization ratio at 355nm (VDR355), rather than on particle backscatter coefficients (BSC355) and particle depolarization ratios (PDR355). These quantities BSC355 and PDR355 would allow a much better and more clear interpretation of the observations.

The use of VDR355 means that any variation in VDR355 may be partly related to (a) changes in the particle-to-molecular backscatter ratio and (b) changes in the ratio of non-depolarizing droplets to depolarizing ice crystals. This ambiguity must be considered in the entire discussion. This ist not the case in the present version of the paper. This has to be improved.

As can be seen from my quite long list of remaining comments and questions, we need another round of revision.

Authors' response:

The authors sincerely thank this reviewer for alerting us to the difference between the volume depolarization ratio δ_v /attenuated backscatter coefficient and the particle depolarization ratio δ_p/particle backscatter coefficient in interpretating the lidar-observed cloud/virga results. In order to clarify this issue, please allow us to examine the functional dependence of δ_p (PDR355) upon δ_v (VDR355) and upon lidar backscattering ratio R ($R(z) = \frac{\beta_a(z)+\beta_m(z)}{\beta_m(z)}$) based on the polarization lidar measurements from both our current study and earlier literatures. The particle depolarization ratio (δ_p) can be obtained from the following equation (Cairo et al., AO, 1999):

$$\delta_p(z) = \frac{(1+\delta_m)\delta_v(z)R(z) - \left(1+\delta_v(z)\right)\delta_m}{(1+\delta_m)R(z) - \left(1+\delta_v(z)\right)}, \qquad (1)$$

where δ_m is the molecular depolarization ratio. In light of the theoretical calculation by Behrendt and Nakamura (OE, 2002), the δ_m value is ~0.004 for our 0.3-nm bandwidth polarization lidar (355 nm). We have historically measured a minimum depolarization ratio of 0.0067 in clear air as shown by the following Figure R1. The small depolarization excess (0.0027, exceeding the theoretical δ_m value of 0.004) can be ascribed to a small remaining ellipticity in the optics or stress birefringence in our waterproof transparent roof windows.

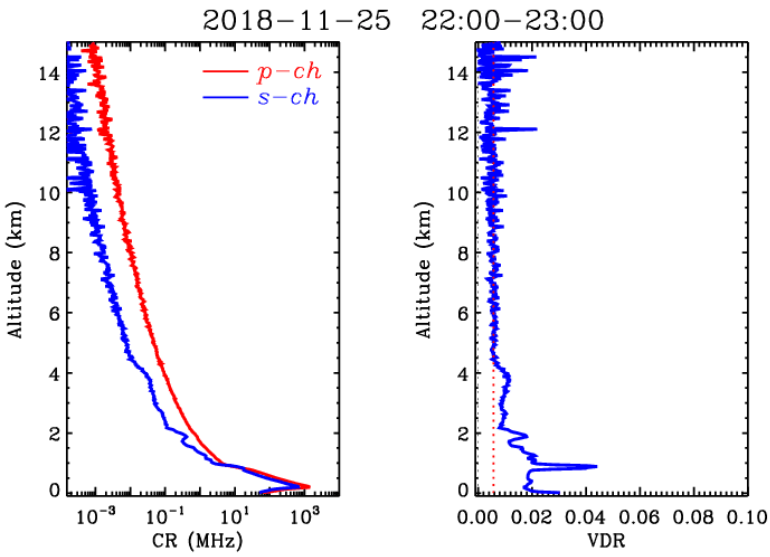

Figure R1. The minimum volume depolarization ratio (VDR, red dotted line in the right panel) in clear air measured by our 355-nm polarization lidar.

Figure R2 illustrates the functional relationship between the derived particle depolarization ratio δ_p (from Equation (1)) and lidar-measured volume depolarization ratio δ_v for three specified lidar backscattering ratio (*R*) values. The *R* values are fixed by considering the earlier lidar measurements. Specifically, the typical values of *R* for enhanced aerosol load are around 2, for optically thin clouds up to around 10 (please see Lampert et al., ACP, 2010, p2849). The *R* values were ~5–8 on the upper part of evaporating shallow (~400-m thick) ice virgae (please see Figure 4 in (Cheng and Yi, RS, 2020)). Thus, it is reasonable to set a *R* value of at least 7 for the precipitation-related virgae shown in Figs.4-6 and Figs.9-10 in the revised manuscript because this type of the virga layers is more than 2-km thick with an ice/snow bright band above and a liquid-water bright band below (separated by a lidar dark band). As seen from Figure R2, for the fixed lidar backscatter ratios (*R*=5,7,10), the functional dependence of δ_p (PDR355) on δ_v (VDR355) is quasilinear with a zero offset and an apparent slope slightly larger than 1 (the nonlinear term belongs to high-order small quantity) in conventional polarization lidar measurement range (δ_v~0–0.6). This is a mathematical basis for the δ_v (VDR355) to discriminate whether the dominant lidar backscattering is attributed to spherical or nonspherical particles in a given backscatter volume (or altitude). The δ_p magnitude is always slightly larger than the corresponding lidar-measured δ_v value with the net increment ($\delta_p - \delta_v$) being small in the low-δ_v-value range ($\delta_v < 0.1$), and being relatively large in the high-δ_v-value range (e.g., $\delta_v > 0.3$). The magnitude of the net increment decreases with increasing R value.

Figure R2 enables us to obtain the discrimination criteria of water droplets and ice crystals expressed by the magnitudes of the volume depolarization ratio for a fixed R value. If the discrimination criterion of water droplets is defined as $\delta_p < 0.1$ in terms of the particle depolarization ratio δ_p when $R = 7$, the equivalent criterion is $\delta_v <0.09$ in terms of the volume depolarization ratio δ_v. If the discrimination criterion of ice crystals is defined as $\delta_p > 0.2$ in terms of the particle depolarization ratio δ_p when R=7, the equivalent criterion is $\delta_v > 0.17$ in terms of the volume depolarization ratio δ_v.

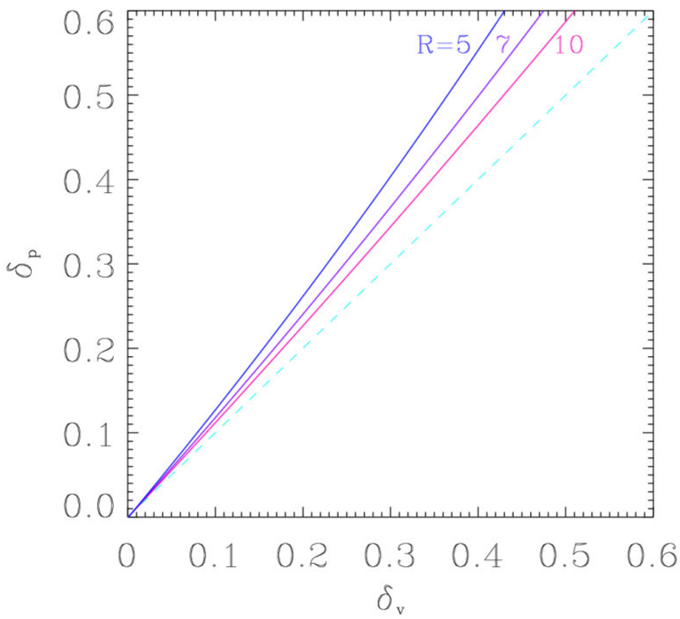

Figure R2. The particle depolarization ratio (δ_p) as a function of the lidar-measured volume depolarization ratio (δ_v) for specified lidar backscattering ratio (R) values (R ≥ 7 is suitable for the precipitation-related virga in this study). The cyan dashed line denotes a linear function with a slope value of 1.0.

In order to further clarify whether the δ_v (VDR355) magnitude is valid in discriminating spherical or nonspherical particles in a given backscatter volume (or altitude) for the present study, according to Equation (1), we analyse now the particle depolarization ratio δ_p as a function of lidar backscatter ratio R for fixed δ_v values that are from our current lidar observations.

As the first example in this study, let us see whether the change in the δ_v values of falling hydrometeors during the first 100–200 m of their descent coincides with the δ_p variation (from the liquid-water values to the ice/snow values). On 28 Dec 2017, the lidar-measured δ_v had the mean values of ~0.059 at 4.35-km altitude and ~0.037 at 4.38 km (on the ice virga top, please see Fig.6b in the revised manuscript). Inserting the two δ_v values (as parameters) into Equation (1), the δ_p (PDR355) is calculated as a function of R (plotted in Figure R3). As seen in Figure R3, all the δ_p values on the curves for δ_v =0.059 and δ_v =0.037 are smaller than 0.1 in the entire range of possible R values (7-100, the R values should be larger than 7 for the precipitation-related virga). The maximum δ_p values on the curves are respectively 0.069 at 4.35-km altitude and 0.042 at 4.38 km (corresponding to R=7), indicating that the dominant lidar backscattering should be attributed to spherical water drops/droplets at these altitudes.

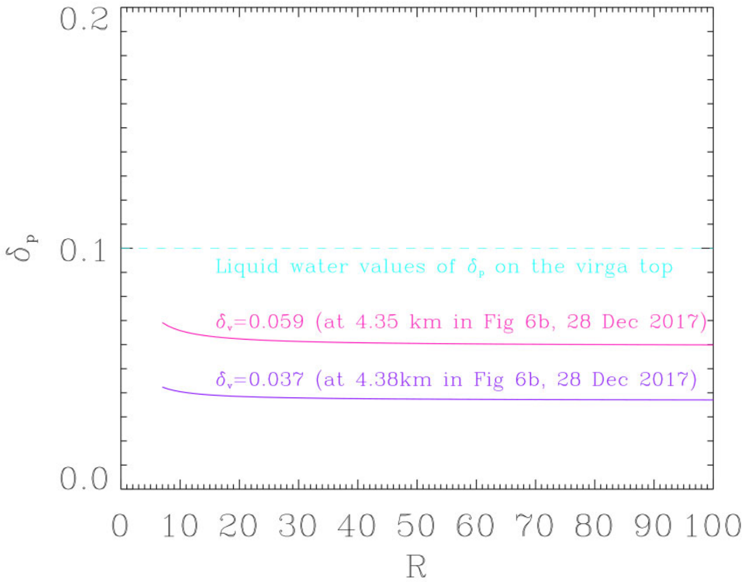

Figure R3. The δ_p (PDR355) as a function of lidar backscatter ratio R for the lidar-measured volume depolarization ratio δ_v (VDR355) values at two different altitudes (Fig. 6b in the revised manuscript, 28 Dec 2017). The δ_v =0.059 and δ_v =0.037 are the average values at 4.35-km and 4.38-km altitudes respectively. Note that all the δ_p values on the curves for δ_v =0.059 and δ_v =0.037 (at the ice virga top) are clearly less than 0.1 in the entire range of possible R values (7-100).

On the same day (28 Dec 2017), the lidar-measured δ_v had the mean values of ~0.220 at 4.17-km altitude and ~0.259 at 4.02 km (at altitudes ~180–330 m below the the ice virga top, please see Fig.6b in the revised manuscript). Inserting the two δ_v values (as parameters) into Equation (1), the δ_p (PDR355) is calculated as a function of R (plotted in Figure R4). As seen in Figure R4, all the δ_p values on the curves for δ_v =0.220 and δ_v =0.259 are larger than 0.2 in the entire range of possible R values (7-100, the R values should be larger than 7 for the precipitation-related virga). The minimum δ_p values on the curves are respectively 0.223 at 4.17-km altitude and 0.262 at 4.02 km (corresponding to R=100), indicating that the dominant lidar backscattering should be attributed to nonspherical ice crystals at these altitudes.

Figure R3 and R4 indicate that the δ_p (PDR355) magnitude is mainly controlled by the δ_v (VDR355) magnitude (low and high values), and has a very weak dependence on lidar backscatter ratio R (when $R \geq 7$). Hence the conclusion "The depolarization ratio magnitude of falling hydrometeors increased from the liquid-water values (δ_v< 0.09) to the ice/snow values (δ_v> 0.20) during the first 100–200 m of their descent" (P17, l515) should be valid.

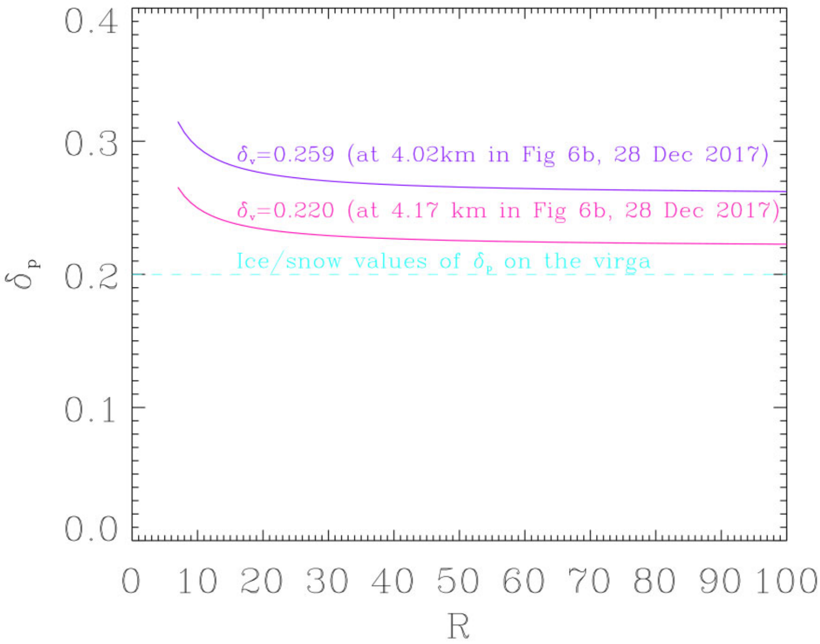

Figure R4. The δ_p (PDR355) as a function of lidar backscatter ratio R for the lidar-measured volume depolarization ratio δ_v (VDR355) values at two different altitudes (Fig. 6b in the revised manuscript, 28 Dec 2017). The δ_v =0.220 and δ_v =0.259 are the average values at 4.17-km and 4.02-km altitudes respectively. Note that all the δ_p values on the curves for δ_v =0.220 and δ_v =0.259 (at altitudes ~180–330 m below the ice virga top) are clearly larger than 0.2 in the entire range of possible R values (7-100).

As the second example in this study, we examine for the water bright band, whether the low δ_v (VDR355) values correspond to the low δ_p (PDR355) values, and the high δ_v (VDR355) values correspond to the high δ_p (PDR355) values when the lidar backscatter ratio R varies in the range of all possible R values. As seen in Figure 10b in the revised manuscript, "in the height range of the water bright band, the depolarization ratio (δ_v) increased from ~0.04–0.06 at an altitude of approximately 2.09 km to ~0.12–0.15 at an altitude of 0.9 km, indicating that more large raindrops formed via collision-coalescence processes therein" (please see P15-16, l471-474). Similarly, inserting the two δ_v mean values (0.05 and 0.135) into Equation (1), the δ_p (PDR355) is calculated as a function of R (plotted in Figure R5). As seen in Figure R5, all the δ_p values on the curve for δ_v =0.135 are obviously larger than those on the curve for δ_v =0.05 in the entire range of possible R values (3-100), indicating that the low δ_v (VDR355) value does correspond to the low δ_p (PDR355) value, and the high δ_v (VDR355) value does correspond to the high δ_p (PDR355) value when the lidar backscatter ratio R varies in the range of all possible R values.

In light of our numerical analysis (particularly about the δ_p (PDR355) as a function of lidar backscatter ratio R for fixed volume depolarization ratio δ_v (VDR355) values from our lidar observations), all the δ_v-based discussions in this paper are valid.

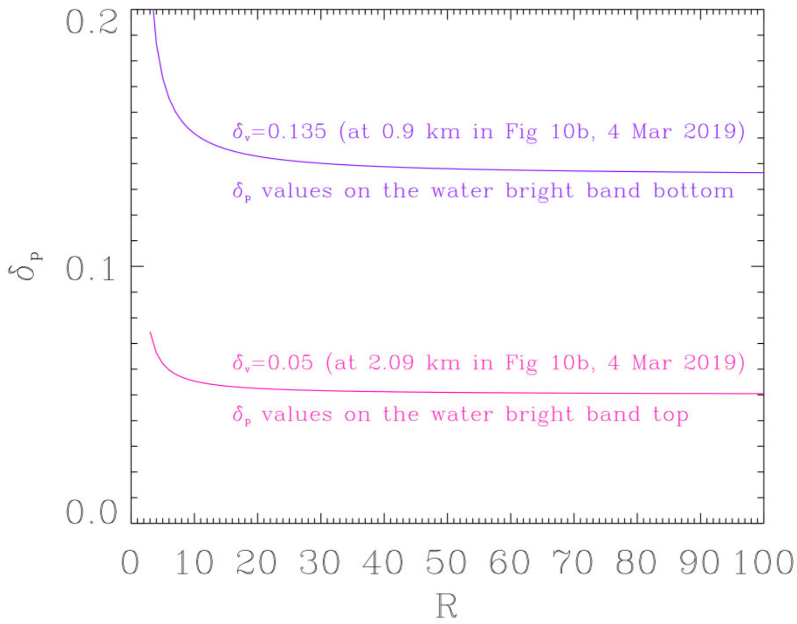

Figure R5. The δ_p (PDR355) as a function of lidar backscatter ratio R for the lidar-measured volume depolarization ratio δ_v (VDR355) values at two different altitudes (please see Fig. 10b in the revised manuscript, 4 Mar 2019). The δ_v =0.05 and δ_v =0.135 are the average values at 2.09-km and 0.9-km altitudes respectively. Note that all the δ_p values for δ_v =0.135 (at the water bright band bottom) are obviously larger than those for δ_v =0.05 (at the water bright band top) in the entire range of possible R values (3-100).

The numerical results shown in Figures R2-R5 can be addressed also by mathematically analyzing Equation (1). Because the molecular depolarization ratio ($\delta_m(0.004)$<< 1) can be neglected, the Equation (1) is reduced to the following form

$$\delta_p(\mathrm{z}) = \frac{1}{1-\frac{1+\delta_v(\mathrm{z})}{R(z)}}\delta_v(\mathrm{z}). \quad (2)$$

As seen from the Equation (2), when R(z) > 5, the particle depolarization ratio δ_p (PDR355) has a very weak dependence on the lidar backscatter ratio R (via factor $\frac{1}{1-\frac{1+\delta_v(\mathrm{z})}{R(z)}}$), and then a quasilinear dependence on the volume depolarization ratio δ_v (VDR355). This is consistent with the result shown in Figure R2. In more detail, for precipitation-related cloud/virga in this study, R >7, a Tailor series expansion of Equation (2) yields

$$\delta_p(\mathrm{z}) \approx (1+\frac{1}{R(z)}+\frac{\delta_v(\mathrm{z})}{R(z)})\delta_v(\mathrm{z}). \quad (3)$$

The first two terms on the right-hand side of Equation (3) describe a linear dependence of $\delta_p(\mathrm{z})$ on $\delta_v(\mathrm{z})$ with a slope of $1+\frac{1}{R(z)}$, indicating that the $\delta_p(\mathrm{z})$

magnitude is slightly larger than the lidar-measured $\delta_v(\mathrm{z})$ value because $\frac{1}{R(z)}$ <<1 as R > 7. The third term $\frac{\delta_v(\mathrm{z})}{R(z)}\delta_v(\mathrm{z})$ is a nonlinear modification to the δ_p-δ_v relationship, that is smaller in magnitude than the second term $\frac{\delta_v(\mathrm{z})}{R(z)}$.

According to Equation (2), we can respectively derive the discrimination criteria of spherical and nonspherical particles expressed by the lidar-measured volume depolarization ratio based on those defined by the particle depolarization ratio δ_p. For the purpose, we examine now the particle depolarization ratio δ_p as a function of lidar backscatter ratio R for fixed δ_v values that are from our current lidar observations. In light of the previous observations, particles with $\delta_p < 0.1$ can be discriminated as spherical particles (Intrieri et al., 2002; Ansmann et al., 2008) and particles with $\delta_p > 0.2$ can be unquestionably discriminated as nonspherical particles (Wang and Sassen, 2001). In terms of Equation (2), the discrimination threshold value of spherical particles is written as

$$\frac{1}{1-\frac{1+\delta_v(\mathrm{z})}{R(z)}}\delta_v(\mathrm{z}) = 0.1,\ \text{i.e.}\ \delta_p(\mathrm{z}) = 0.1,\ (4)$$

which is equivalent to

$$\delta_{v,\mathrm{threshold}}(R) = 0.1 - \frac{0.11}{R+0.1}.\quad (5)$$

The lidar backscatter ratio R has a theoretical value range of $[R_{\min}, \infty)$ with $R_{\min}$ being the minimum possible value of R for the interested clouds/virgae (e.g., $R_{\min}$=7 for the precipitation-related virgae). The corresponding $\delta_{v,\mathrm{threshold}}$ has a value range of $[0.1 - \frac{0.11}{R_{\min}+0.1}, 0.1)$. Hence, the discrimination criterion of spherical particles expressed by $\delta_v(\mathrm{z})$ has the following form

$$\delta_v(\mathrm{z}) < 0.1 - \frac{0.11}{R_{\min}+0.1}.\quad (6)$$

Inserting $R_{\min}$=7 (for the precipitation-related virgae) into (6), we have

$$\delta_v(\mathrm{z}) < 0.085.$$

This δ_v threshold value (0.085) of spherical particles is close to that value of 0.9 from the above strict calculation based on Equation (1). When $R_{\min}$=5, we have

$$\delta_v(\mathrm{z}) < 0.078.$$

In terms of Equation (2), the discrimination threshold value of nonspherical particles is given by

$$\frac{1}{1-\frac{1+\delta_v(z)}{R(z)}}\delta_v(z) = 0.2, \text{ i.e.} \delta_p(z) = 0.2, \quad (7)$$

which is equivalent to

$$\delta_{v,\text{threshold}}(R) = 0.2 - \frac{0.24}{R + 0.2}. \quad (8)$$

The lidar backscatter ratio R has a theoretical value range of $[R_{\min}, \infty)$ with $R_{\min}$ being the minimum possible value of R for the interested clouds/virgae (e.g., $R_{\min}=7$ for the precipitation-related virgae). The corresponding $\delta_{v,\text{threshold}}$ has a value range of $[0.2 - \frac{0.24}{R_{\min}+0.2}, 0.2)$. Since $\delta_{v,\text{threshold}}(R)$ is a slowly-varying function of R as seen from Equation (8) (particularly when $R_{\min} \geq 5$), the discrimination criterion of nonspherical particles expressed by $\delta_v(z)$ can be written approximately as

$$\delta_v(z) > 0.2 - \frac{0.24}{R_{\min} + 0.2}. \quad (9)$$

When $R_{\min}=7$, the discrimination criterion of nonspherical particles is given by

$$\delta_v(z) > 0.167,$$

which is equivalent to $\delta_p(z) > 0.2$ approximately.

In conclusion, the particle depolarization ratio δ_p (PDR355) has a quasilinear dependence on the volume depolarization ratio δ_v (VDR355), and a very weak dependence on lidar backscatter ratio R (when $R \geq 5$). This favorable functional dependence allows us to utilize δ_v (VDR355) in discriminating whether the dominant lidar backscattering is attributed to spherical or nonspherical particles in a given backscatter volume. If $R_{\min}$ is the minimum of the R value range for the interested clouds/virgae (e.g., $R_{\min}=7$ for the precipitation-related virgae), the discrimination criterion of spherical particles expressed by $\delta_v(z)$ has the following form

$$\delta_v(z) < 0.1 - \frac{0.11}{R_{\min} + 0.1},$$

while the discrimination criterion of nonspherical particles expressed by $\delta_v(z)$ is given approximately by

$$\delta_v(z) > 0.2 - \frac{0.24}{R_{\min} + 0.2}.$$

Based on the analysis and discussion above, we have added a new paragraph and an Appendix in the second-round-revised manuscript.

“It is should be mentioned that the particle depolarization ratio δ_p is conceptually a more suitable quantity in discriminating spherical and nonspherical particles (hydrometeors) in virga/cloud than the volume depolarization ratio δ_v. But, the volume depolarization ratio δ_v represents the more basic lidar measurement. In order to validly utilize the δ_v magnitude in discriminating spherical and nonspherical depolarizations, we have examined the relationship between δ_p and δ_v. The δ_p magnitude is a well-defined function of δ_v, lidar backscattering ratio R and molecular depolarization ratio δ_m (Cairo et al., 1999). The molecular depolarization ratio δ_m has a value of ~0.004 in terms of our lidar receiver bandwidth (0.3 nm) (Behrendt and Nakamura, 2002). Information about the R value range is available from a combined consideration of the earlier lidar measurements and our current observations on precipitation-related cloud/virga. The typical values of R for enhanced aerosol load are around 2, for optically thin clouds up to around 10 (Lampert et al., 2010). The R values are ~5−8 on the upper part of typical shallow (~400-m thick) evaporating ice virgae (see Figure 4 in (Cheng and Yi, 2020)). In this study, the R value should certainly be larger than 7 on the precipitation-related virga layer. Based on the analysis to the δ_p expression (Cairo et al., 1999) for clouds and virgae, the particle depolarization ratio δ_p has a quasilinear dependence on the volume depolarization ratio δ_v, and a very weak dependence on lidar backscatter ratio R (when $\mathrm{R} \geq 5$). This favorable feature of the functional dependences allows us to utilize δ_v in discriminating whether the dominant lidar backscattering is attributed to spherical or nonspherical particles in a given backscatter volume. If $R_{\min}$ is the minimum of the R value range for the interested clouds/virgae (e.g., $R_{\min} = 7$ for the precipitation-related virgae in this study), the discrimination criterion of spherical particles expressed by $\delta_v(\mathrm{z})$ (equivalent to $\delta_p < 0.1$) takes the form (see Appendix A for mathematical derivation)

$$\delta_v(\mathrm{z}) < 0.1 - \frac{0.11}{R_{\min} + 0.1} \,. \qquad (1)$$

The discrimination criterion of nonspherical particles expressed by $\delta_v(\mathrm{z})$ (equivalent to $\delta_p > 0.2$) is given approximately by

$$\delta_v(\mathrm{z}) > 0.2 - \frac{0.24}{R_{\min} + 0.2} \,. \qquad (2)$$

As noticed from the right-hand sides of Inequalities (1) and (2), the absolute differences between the discrimination threshold values expressed by δ_p (0.1 and 0.2) and by δ_v are small for clouds/virgae with $R_{\min} > 7$. The unambiguous cloud-phase discriminations based on the volume depolarization ratio δ_v in earlier literatures (Wang and Sassen, 2001; Intrieri et al., 2002; Shupe, 2007; Ansmann et al., 2009; Lampert et al., 2010) have confirmed the functional relationship between δ_p and δ_v mentioned above. This allows us to employ δ_v with very little threshold-value change in discriminating whether the dominant lidar backscattering is attributed to spherical or nonspherical particles in a given backscatter volume. Specifically, at altitudes above the dark band, the δ_v-based discrimination criteria are $\delta_v < 0.09$ for spherical water drops/droplets and $\delta_v > 0.17$ for ice crystals (based on the above discrimination criteria when $R_{\min} = 7$), while an enhanced depolarization ratio ($\delta_v > 0.1$) at altitudes below the dark band indicates the presence of large raindrops." （please see P4-5, l115-148）

Appendix A: Discrimination criteria of spherical and nonspherical particles based on volume depolarization ratio

Here we derive the equivalent results expressed by the volume depolarization ratio δ_v based on the discrimination criteria of spherical and nonspherical particles given by the particle depolarization ratio δ_p. The particle depolarization ratio δ_p can be obtained from the following equation (Cairo et al., 1999):

$$\delta_p(\mathrm{z}) = \frac{(1+\delta_m)\delta_v(\mathrm{z})R(z) - \left(1+\delta_v(\mathrm{z})\right)\delta_m}{(1+\delta_m)R(z) - \left(1+\delta_v(\mathrm{z})\right)}, \qquad \text{(A1)}$$

where δ_m is the molecular depolarization ratio and $R(z)$ the lidar backscatter ratio. In light of the theoretical calculation by Behrendt and Nakamura (2002), the δ_m value is ~0.004 for our 0.3-nm bandwidth polarization lidar (355 nm). Because the molecular depolarization ratio ($\delta_m(0.004) \ll 1$) can be neglected, the Eq. A1 is reduced to the following form

$$\delta_p(\mathrm{z}) = \frac{1}{1 - \frac{1+\delta_v(\mathrm{z})}{R(z)}}\delta_v(\mathrm{z}). \quad \text{(A2)}$$

According to Eq. A2, we can respectively derive the discrimination criteria of spherical and nonspherical particles expressed by the lidar-measured volume depolarization ratio δ_v based on those defined by the particle depolarization ratio δ_p. In light of the previous observations, particles with $\delta_p < 0.1$ can be discriminated as spherical particles (Intrieri et al., 2002; Ansmann et al., 2008) and particles with $\delta_p > 0.2$ can be unquestionably discriminated as nonspherical particles (Wang and Sassen, 2001). In terms of Eq. A2, the discrimination threshold value of spherical particles takes the form

$$\frac{1}{1 - \frac{1+\delta_v(\mathrm{z})}{R(z)}}\delta_v(\mathrm{z}) = 0.1, \qquad \text{i.e.}, \delta_p(\mathrm{z}) = 0.1, \qquad \text{(A3)}$$

which is equivalent to

$$\delta_{v,\text{threshold}}(R) = 0.1 - \frac{0.11}{R + 0.1}. \qquad \text{(A4)}$$

The lidar backscatter ratio R has a theoretical value range of $[R_{\min}, \infty)$ with $R_{\min}$ being the minimum possible value of R for the interested clouds/virgae (e.g., $R_{\min} = 7$ for the precipitation-related virgae). The corresponding $\delta_{v,\text{threshold}}$ has a value range of $\left[0.1 - \frac{0.11}{R_{\min}+0.1}, 0.1\right)$. Hence, the discrimination criterion of spherical particles expressed by $\delta_v(\text{z})$ has the following form

$$\delta_v(\text{z}) < 0.1 - \frac{0.11}{R_{\min} + 0.1}. \qquad \text{(A5)}$$

Inserting $R_{\min} = 7$ (for the precipitation-related virgae) into Eq. A5, we have $\delta_v(\text{z}) < 0.085$. This δ_v threshold value (0.085) of spherical particles is close to that value of 0.9 from the strict calculation based on Eq. A1. When $R_{\min} = 5$, we have $\delta_v(\text{z}) < 0.078$.

In terms of Eq. A2, the discrimination threshold value of nonspherical particles is given by

$$\frac{1}{1 - \frac{1 + \delta_v(\text{z})}{R(z)}} \delta_v(\text{z}) = 0.2, \qquad \text{i.e.}, \delta_p(\text{z}) = 0.2, \qquad \text{(A6)}$$

which is equivalent to

$$\delta_{v,\text{threshold}}(R) = 0.2 - \frac{0.24}{R + 0.2}. \qquad \text{(A7)}$$

The lidar backscatter ratio R has a theoretical value range of $[R_{\min}, \infty)$ with $R_{\min}$ being the minimum possible value of R for the interested clouds/virgae (e.g., $R_{\min} = 7$ for the precipitation-related virgae). The corresponding $\delta_{v,\text{threshold}}$ has a value range of $[0.2 - \frac{0.24}{R_{\min}+0.2}, 0.2)$. Since $\delta_{v,\text{threshold}}(R)$ is a slowly-varying function of R as seen from Eq. A7 (particularly when $R_{\min} \geq 5$), the discrimination criterion of nonspherical particles expressed by $\delta_v(\text{z})$ can be written approximately as

$$\delta_v(\text{z}) > 0.2 - \frac{0.24}{R_{\min} + 0.2}. \qquad \text{(A8)}$$

When $R_{\min} = 7$, the discrimination criterion of nonspherical particles is given by $\delta_v(\text{z}) > 0.167$, which is equivalent to $\delta_p(\text{z}) > 0.2$ approximately.

In conclusion, the particle depolarization ratio δ_p has a quasilinear dependence on the volume depolarization ratio δ_v, and a very weak dependence on lidar backscatter ratio R (when $R \geq 5$). This favorable functional dependence allows us to utilize δ_v in discriminating whether the dominant lidar backscattering is attributed to spherical or nonspherical particles in a given backscatter volume. If $R_{\min}$ is the minimum of the R value range for interested clouds/virgae (e.g., $R_{\min} = 7$ for the precipitation-related virgae), the discrimination criterion of spherical particles expressed by $\delta_v(\mathrm{z})$ is given by Eq. A5, while the discrimination criterion of nonspherical particles expressed by $\delta_v(\mathrm{z})$ is given approximately by Eq. A8.

The manuscript has been further revised by taking all the comments (in the Details) into account.

References added

Behrendt, A. and Nakamura, T.: Calculation of the calibration constant of polarization lidar and its dependency in atmospheric temperature, Optics Express, 10 (16), https://doi.org/10.1364/OE.10.000805, 2002.

Cairo, F., Donfrancesco, G. D., Adriani, A., Pulvirenti, L., and Fierli, F.: Comparison of various linear depolarization parameters measured by lidar, Appl. Opt., 38, 4425–4432, https://doi.org/10.1364/AO.38.004425, 1999.

Lampert, A, Ritter, C., Hoffmann, A. Gayet, J.-F., Mioche, G., Ehrlich, A., Dörnbrack, A., Wendisch, M., and Shiobara, M.: Lidar characterization of the Arctic atmosphere during ASTAR 2007: four cases studies of boundary layer, mixed-phase and multi-layer clouds, Atmos. Chem. Phys., 10, 2847–2866, https://doi.org/10.5194/acp-10-2847-2010, 2010.

Comments:

P1 l20: the authors write: …the depolarization ratio of falling hydrometeors increases from liquid-water values to the ice/snow values… My question: How do you know that this is related to the changing ratio of droplet-to-crystal number concentration? As mentioned above, VDR355 is used and depends on Rayleigh depolarization (causes a depolarization ratio of about 0.01). The lower BSC355 (or attenuated backscatter), the lower VDR355. And vice versa, the higher BSC355, the higher VDR355. This can be simply caused by the decreasing impact of Rayleigh backscattering on VDR355 with increasing BSC355.

So please keep that in mind and improve the text accordingly.

Authors' response:

As mentioned by Ansmann et al. (JGR, 2009), "The sensitivity of a polarization lidar is not high enough to detect a few ice crystals in a liquid layer or a few droplets in ice virga. The advantage of active remote sensing is to visualize the vertical context..." (please see page 19 in (Ansmann et al., JGR, 2009)). In other words, a polarization lidar can discriminate whether the dominant lidar backscattering is attributed to ice crystals or water droplets in a given backscatter volume of cloud/virga (at a given altitude) rather than detect the ratio of droplet-to-crystal number concentration.

First, in light of the δ_p-based discrimination criteria ($\delta_p < 0.1$ for water droplets, and $\delta_p > 0.2$ for ice crystals), let us see whether the change in the δ_v values of falling hydrometeors during the first 100–200 m of their descent coincides with the expected δ_p variation (from the liquid-water values to the ice/snow values). For this purpose, we start with the previous Equation (1) (Cairo et al., AO, 1999)

$$\delta_p(\mathrm{z}) = \frac{(1+\delta_m)\delta_v(\mathrm{z})R(z)-(1+\delta_v(\mathrm{z}))\delta_m}{(1+\delta_m)R(z)-(1+\delta_v(\mathrm{z}))}, \ \delta_m = 0.004. \quad (1)$$

On 28 Dec 2017, the lidar-measured δ_v had the mean values of ~0.059 at 4.35-km altitude and ~0.037 at 4.38 km (on the ice virga top, please see Fig.6b in the revised manuscript). Inserting the two δ_v values (as parameters) into Equation (1), the δ_p (PDR355) is calculated as a function of R (plotted in Figure R3). As seen in Figure R3, all the δ_p values on the curves for δ_v =0.059 and δ_v =0.037 are smaller than 0.1 in the entire range of possible R values (7-100, the R values should be larger than 7 for the precipitation-related virga). The maximum δ_p values on the curves are respectively 0.069 at 4.35-km altitude and 0.042 at 4.38 km (corresponding to R=7), indicating that the dominant lidar backscattering should be attributed to spherical water drops/droplets at these altitudes.

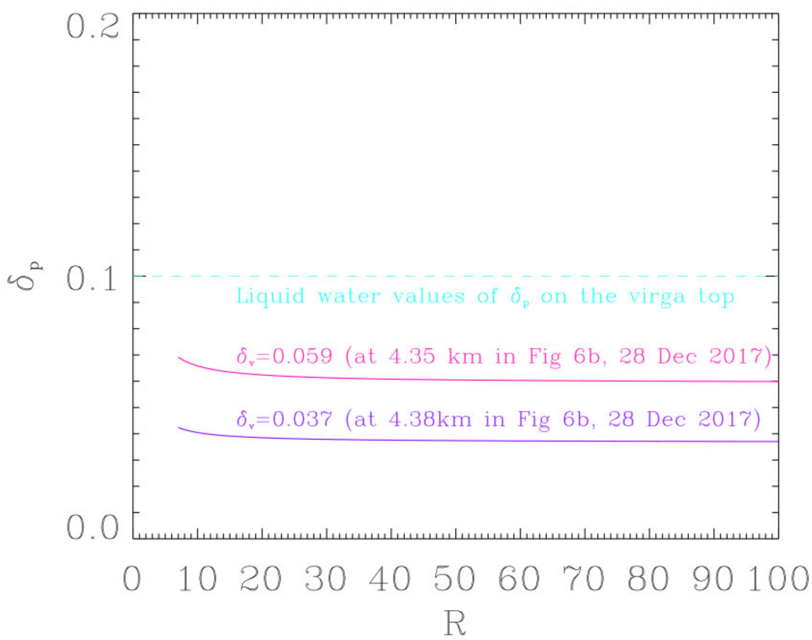

Figure R3. The δ_p (PDR355) as a function of lidar backscatter ratio R for the lidar-measured volume depolarization ratio δ_v (VDR355) values at two different altitudes (Fig. 6b in the revised manuscript, 28 Dec 2017). The δ_v =0.059 and δ_v =0.037 are the average values at 4.35-km and 4.38-km altitudes respectively. Note that all the δ_p values on the curves for δ_v =0.059 and δ_v =0.037 (at the ice virga top) are clearly less than 0.1 in the entire range of possible R values (7-100).

On the same day (28 Dec 2017), the lidar-measured δ_v had the mean values of ~0.220 at 4.17-km altitude and ~0.259 at 4.02 km (at altitudes ~180–330 m below the the ice virga top, please see Fig.6b in the revised manuscript). Inserting the two δ_v values (as parameters) into Equation (1), the δ_p (PDR355) is calculated as a function of R (plotted in Figure R4). As seen in Figure R4, all the δ_p values on the curves for δ_v =0.220 and δ_v =0.259 are larger than 0.2 in the entire range of possible R values (7-100, the R values should be larger than 7 for the precipitation-related virga). The minimum δ_p values on the curves are respectively 0.223 at 4.17-km altitude and 0.262 at 4.02 km (corresponding to R=100), indicating that the dominant lidar backscattering should be attributed to nonspherical ice crystals at these altitudes.

Figures R3 and R4 indicate that the δ_p (PDR355) magnitude is mainly controlled by the δ_v (VDR355) magnitude (low and high values), and has a very weak dependence on lidar backscatter ratio R (when $R \geq 7$). Hence the conclusion "The depolarization ratio magnitude of falling hydrometeors increased from the liquid-water values ($\delta_v < 0.09$) to the ice/snow values ($\delta_v > 0.20$) during the first 100–200 m of their descent" (P1, l20) is correct unambiguously.

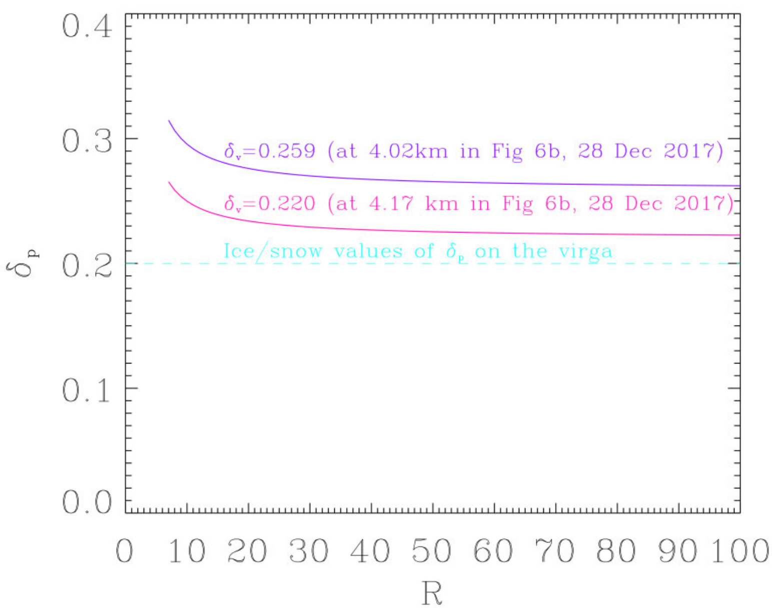

Figure R4. The δ_p (PDR355) as a function of lidar backscatter ratio R for the lidar-measured volume depolarization ratio δ_v (VDR355) values at two different altitudes (Fig. 6b in the revised manuscript, 28 Dec 2017). The δ_v =0.220 and δ_v =0.259 are the average values at 4.17-km and 4.02-km altitudes respectively. Note that all the δ_p values on the curves for δ_v =0.220 and δ_v =0.259 (at altitudes ~180–330 m below the ice virga top) are clearly larger than 0.2 in the entire range of possible R values (7-100).

On the other hand, the δ_v-based discrimination criteria derived above also allow us to discriminate between water droplets and ice crystals. Their expressions are given by:

$$\delta_v(\mathrm{z}) < 0.1 - \frac{0.11}{R_{\min}+0.1} \text{ for water droplets,} \quad (6)$$

$$\delta_v(\mathrm{z}) > 0.2 - \frac{0.24}{R_{\min}+0.2} \text{ for ice crystals,} \quad (9)$$

where $R_{\min}$ is the minimum of the R value range for the interested clouds/virgae. For the precipitation-related virgae shown in Fig.6b in the revised manuscript, we take $R_{\min}$ =7. Thus the δ_v-based discrimination criteria become

$$\delta_v(\mathrm{z}) < 0.085 \text{ for water droplets,}$$

$$\delta_v(\mathrm{z}) > 0.167 \text{ for ice crystals.}$$

The lidar-measured δ_v had the mean values of ~0.059 at 4.35-km altitude and ~0.037 at 4.38 km (on the ice virga top, please see Fig.6b in the revised manuscript). Both the values were less than the δ_v-based water-droplet discrimination threshold 0.085, indicating that the dominant lidar backscattering was attributed to spherical water drops on the ice virga top. The lidar-measured δ_v had the mean values of ~0.220 at 4.17-km altitude and ~0.259 at 4.02 km (at altitudes ~180–330 m below the the ice virga top, please see Fig.6b in the revised manuscript). Both the values were larger than the δ_v-based ice-crystal discrimination threshold 0.167, indicating that the dominant lidar backscattering was attributed to ice crystals at the slightly lower altitudes.

Comments:

P2, l54-55: The authors write: ..revealed the detailed vertical structures of falling mixed-phase virga…. Again, with VDR355, you are not able to give clear answers. Only with PDR355 you would be able to do that.

By the way, what is a mixed phase virga? A virga consisting of an external mixture of droplets and ice crystals? To my understanding, all virga above the height of the 0°C-level consist of ice crystals. There are no cloud droplets, they are too small to fall out of the cloud deck. Again, the VDR355 probably changes because of the changing Rayleigh backscattering impact.

Authors' response:

In the previous article (Cheng and Yi, Remote Sensing, 2020), we have reported on some ubiquitous vertical structure features of both shallow (~400-m thick) ice virgae and their liquid source cloud layers based on the 3.75-m/1min profiles of lidar backscatter ratio R (not range-corrected signal) and volume depolarization ratio δ_v (VDR532) on 20 occasions (events). Here please allow us to revisit the content of "the detailed vertical structures": Each liquid source cloud had a well-defined base height where the backscatter ratio R was ~7.0 and the R profile had a clear inflection point. At an altitude of ~34 m above the base height, the depolarization ratio reached its minimum value (~0.04), indicating a liquid-only level therein. Below the base height, the δ_v values of falling virgae showed firstly a significant increase with decreasing altitude, after reaching a local maximum, both the values of R and δ_v for the virgae exhibited an overall decrease with decreasing height, indicating sublimated ice crystals. (please see abstract of (Cheng and Yi, Remote Sensing, 2020)). Hence "the detailed vertical structures" in the sentence reflect the real results from our polarization lidar with a high range resolution of 3.75 m. Except that the minimum δ_v value (~0.04) at the altitude ($R \geq 10$) of ~34 m above the base height (R=7) of liquid source clouds changes to δ_p = 0.044 or less (based on the functional relationship between δ_p and δ_v in (Cairo et al., AO, 1999)), all these results are unchanged regardless of whether we utilized δ_v (VDR) or δ_p (PDR).

In light of the mathematical analysis above, the δ_p (PDR) is a quasilinear function of δ_v (VDR) with a zero offset and a slope slightly larger than 1.0, and has a weak dependence on R (via a factor of $\frac{1}{1-\frac{1}{R(z)}}$ roughly) for most clouds ($R \geq 7$) and virgae ($R \geq 5$). According to the lidar-derived R values (~5−8) on the upper part of evaporating shallow (~400-m thick) ice virgae (please see Figure 4 in (Cheng and Yi, RS, 2020)), we assume R= 5 (corresponding to the minimum of the R value range for the shallow ice virgae). Based on the strict functional relationship between δ_p and δ_v (i.e., Equation (1)), the discrimination threshold value of water droplets defined by δ_p (PDR355) ($\delta_{pthreshold}$ = 0.1) becomes $\delta_{vthreshold}$ = 0.08 in terms of δ_v (VDR355) that is only 0.02 smaller than $\delta_{pthreshold}$, while the discrimination threshold value of ice crystals defined by δ_p (PDR355) ($\delta_{pthreshold}$ = 0.2) is equivalent to $\delta_{vthreshold}$ = 0.16. If R= 7, the discrimination threshold value of water droplets ($\delta_{pthreshold}$ = 0.1) is equivalent to $\delta_{vthreshold}$ = 0.09, while the discrimination threshold value of ice crystals ($\delta_{pthreshold}$ = 0.2) is equivalent to $\delta_{vthreshold}$ = 0.17.

Therefore, we can conclude that the favorable functional relationship between δ_p (PDR355) and δ_v (VDR355) enables us to discriminate water droplets and ice crystals in a given backscatter volume of cloud/virga by using δ_v (VDR355). For R values of 5−12, the discrimination criterion of water droplets in terms of δ_v (VDR355) is $\delta_v <$ 0.08−0.09 (corresponding to $\delta_p < 0.1$), while the discrimination criterion of ice crystals is $\delta_v >$ 0.16−0.18 (equivalent to $\delta_p > 0.2$). For R values larger than 12, the discrimination threshold value of water droplets in terms of δ_p (PDR355) is almost the same as that with δ_v (VDR355), the discrimination threshold value of ice crystals in terms of δ_p (PDR355) is only ~0.01 larger than that with δ_v (VDR355). The favorable functional relationship between δ_p and δ_v provides a theoretical basis for the lidar-measured δ_v (VDR355) to discriminate whether the dominant lidar backscattering is attributed to ice crystals or water droplets in a given backscatter volume of cloud/virga (Wang and Sassen, 2001; Intrieri et al., 2002; Shupe, 2007; Ansmann et al., 2009; Lampert et al., 2010).

In the second-round revision, the "...falling mixed-phase virga..." has changed to "...falling virga...". However, with respect to whether all virgae above the height of the 0°C-level consist of ice crystals or not, we have noticed some interesting observational results shown in the earlier literatures. The airborne in-situ measurements show that there sometimes existed detectable liquid water content (LWC) at altitudes of ice virgae (Carey et al., JAMC, 2008, please Figs.1b, 1e-1g).

This can be seen more clearly in the following Figure from the same authors (Niu, Carey et al., conference paper, 2006).

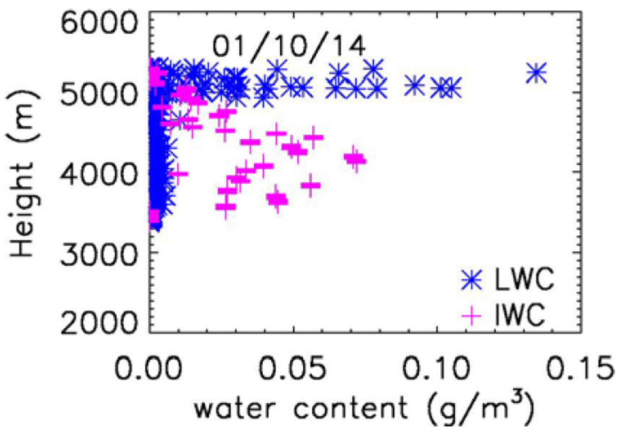

Figure 1. Vertical profile of ice (IWC) and liquid (LWC) water content associated with a common mixed-phase microphysical structure consisting of a super-cooled liquid droplet layer located at the cloud top and ice particles located below. The profile was obtained by the UWKA aircraft beginning at 17:21 UTC on October 14, 2001, just prior to a TERRA/MODIS satellite overpass.

In addition, the drizzle-sized water drop virgae (no ice) were observed beneath thin liquid cloud layers with cloud top temperatures of 0° to –4°C (Rangno and Hobbs, JGR, 2001; Yi et al, AR, 2021), indicating that precipitation-sized particles can form through turbulence (or weak updraft)-induced collision-coalescence process in the thin liquid cloud layers. The similar mechanism should work in an earlier observational example that the virga mainly consisted of drops rather than ice for a moderately supercooled stratiform cloud at temperatures as low as −14°C (Ansmann et al., 2008, please see Fig. 8 and paragraph 52).

References

Carey, L.D., Niu, J., Yang, P., Kankiewicz, J.A., Larson, V.E., Vonder Haar, T.H.: The vertical profile of liquid and ice water content in midlatitude mixed-phase altocumulus clouds, J. Appl. Meteor., 47, 2487-2495, https://doi.org/10.1175/2008JAMC1885.1, 2008.

Niu, J., Carey, L. D., Ping, Y., Kankiewicz, J. A., & Haar, T. A COMMON MICROPHYSICAL STRUCTURE FOR MIDLEVEL MIXED-PHASE CLOUD IN THE MID-LATITUDES: RESULTS FROM THE CLOUD LAYER EXPERIMENT (CLEX-9), 2006.

Rangno, A. L. and Hobbs, P. V.: Ice particles in stratiform clouds in the Arctic and possible mechanisms for the production of high ice concentrations, J. Geophys. Res., 106(D14), 15,065-15,075, https://doi.org/10.1029/2000JD900286, 2001.

Yi, Y., Yi, F., Liu, F., He, Y., Zhang, Y., and Yu, C.: A prolonged and widespread thin mid-level liquid cloud layer as observed by ground-based lidars, radiosonde and space-borne instruments, Atmos. Res., 263, 105815, https://doi.org/10.1016/j.atmosres.2021.105815, 2021.

Comments:
P3, l83: please include after ..... is transmitted vertically into the atmosphere ... (to the zenith).

Authors' response:
The authors thank the reviewer's friendly suggestion. The "(to the zenith)" has been included in the second-round-revised manuscript.

Comments:
P4, L107-110: How do you know about the mixture about droplets and ice crystals? The VDR355 cannot be used to clarify this due to the reasons discussed above. PDR355 would do a better job here.
'Mixed phase' hydrometeors ... Again: What do you mean? ... Internally mixed particles consisting of ice and liquid water? It is certainly an external mixture of droplets and crystals… Again, to my opinion there is only ice in these virga at temperatures below 0°C.

Authors' response:
Here the statement "For some mid-level stratiform precipitations, gravitationally-falling hydrometeors form initially at altitudes above the 0 °C isotherm level. They fall often as mixed-phase hydrometeors (supercooled liquid drops and ice crystals/snowflakes) in sub-zero temperature during their early descent." is based on both existing in-situ and active remote sensing observations rather than simply based on the δ_v (VDR355). As mentioned above, the airborne in-situ measurements show that there sometimes existed detectable liquid water content (LWC) at altitudes of ice virgae (Carey et al., JAMC, 2008, please see Figs.1b, 1e-1g; Niu and Carey et al., conference paper, Fig.1). Observations from both the Lindenberg spectrometric water Raman lidar (Reichardt et al., Accurate absolute measurements of liquid water content (LWC) and ice water content (IWC) of clouds and precipitation with spectrometric water Raman lidar, Journal of Atmospheric and Oceanic Technology, 2021, in press, please see Figure 7) and our spectrometric water Raman lidar have showed the similar result that there was detectable liquid water content in these virgae at temperature below 0°C. An observational example from our spectrometric water Raman lidar is shown in the following Figure R6.

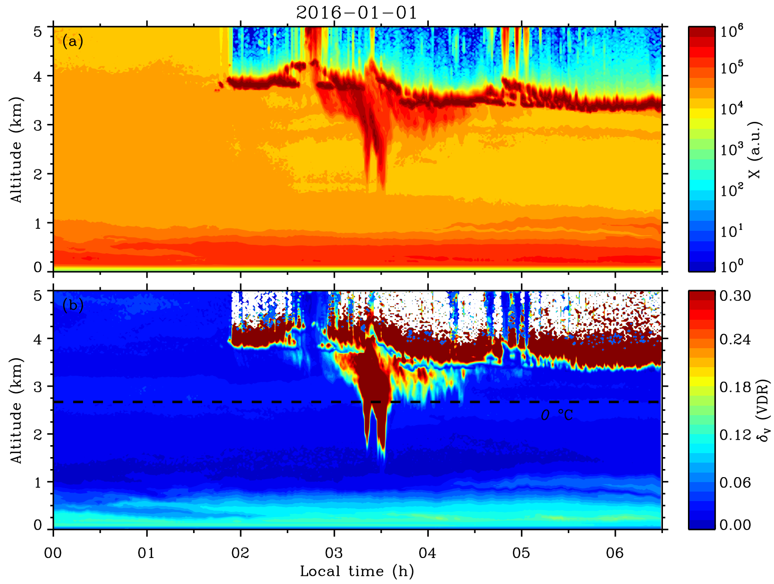

Figure R6A. (a) Range corrected signals X and (b) volume depolarization ratio δ_v (VDR) obtained by our polarization lidar during 0000-0630 LT on 1 January 2016, which show ice virga falling out of a supercooled stratiform cloud. Horizontal dashed line denotes the 0 ℃ level from local radiosonde data at 0800 LT on 1 January 2016.

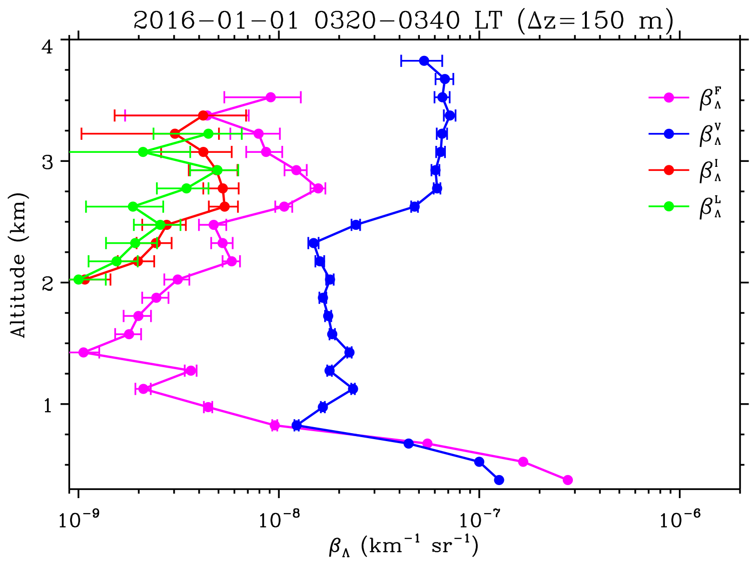

Figure R6B. Profiles of spectrally-integrated total volume backscattering coefficients of fluorescence β_Λ^F (magenta), water vapor β_Λ^V (blue), ice water β_Λ^I (red) and liquid water β_Λ^L (green) retrieved from our spectrometric water Raman lidar measurements during 0320-0340 LT on 1 January 2016 (corresponding to the ice virga shown in Figure R6A). The error bars indicate the 1-σ uncertainties. Note the magnitudes of spectrally-integrated total volume backscattering coefficients $\beta_\Lambda^{V,I,L}$ are respectively proportional to vapor (V), ice (I) and liquid (L) water content.

According to the schematic depiction by Rangno and Hobbs (JGR, 2001, please see Figure 9), the phase state of virgae falling out of stratiform clouds at tempratures below 0°C depends on the cloud top temperature. When the temperature of the cloud top is 0° to −4°C, the virgae consist of only drizzle-sized water drops (no ice). When the temperature of the cloud top is −4° to −10°C, the virgae may be composed of ice crystals and drizzle-sized water drops (please see TYPE III(I) of Figure 9 in (Rangno and Hobbs, JGR, 2001)). For the cloud top temperatures below −10°C, the virga would consist of only ice particles (no supercooled water drops). In practice, Ansmann et al. (JGR, 2008) reported on a lidar-observed example in which the virga mainly consisted of drops rather than ice for a moderately supercooled stratiform cloud at temperatures as low as −14°C (please see Fig. 8 and paragraph 52). A 7-h-lasting water drop virga was observed falling out of an ~0.7-km thick liquid cloud layer at ~3.5-km altitude (Yi et al., AR, 2021). The thin cloud layer resided on an inversion layer with a cloud top temperature of ~−3°C. The temperature of the virga layer ranged from −2° to −3°C because the inversion layer structure existed therein. The two observational examples suggest that water droplets could grow to gravitationally-falling water drops (maybe via turbulence- or weak-updraft-induced collision-coalescence processes) in the liquid stratiform clouds at temperature below 0°C.

Taking the reviewer's comment into account, the statement "They fall often as mixed-phase hydrometeors (supercooled liquid drops and ice crystals/snowflakes) in sub-zero temperature during their early descent." has changed to "They fall often as ice-phase-dominant hydrometeors at sub-zero temperatures during their early descent." (please see P4, lines108-109)

References:

Rangno, A. L. and Hobbs, P. V.: Ice particles in stratiform clouds in the Arctic and possible mechanisms for the production of high ice concentrations, J. Geophys. Res., 106(D14), 15,065-15,075, https://doi:10.1029/2000JD900286, 2001.

Yi, Y., Yi, F., Liu, F., He, Y., Zhang, Y., and Yu, C.: A prolonged and widespread thin mid-level liquid cloud layer as observed by ground-based lidars, radiosonde and space-borne instruments, Atmos. Res., 263, 105815, https://doi.org/10.1016/j.atmosres.2021.105815, 2021.

Comments:

P8, l216-226. This part of the discussion is confusing and speculative and must therefore be changed. You do not know at what height the ice crystals were nucleated! You speculate about the role of contact freezing! There is no observational hint in the literature that contact freezing plays any relevant role! Furthermore, you mention again mixed-phase stratiform precipitation at heights more than 1 km above the 0°C height level. Do you have any measurement that supports all this? As mentioned, VDR355 does not help! So, please remove all the speculative statements.

Here, my most important suggestion to improve the manuscript: On P11, lines 315-321 you provide a perfect explanation of the vertical structure of the cloud-virga system. Therefore: Why not starting the discussion of the lidar observations with Figure 6 (28 Dec, 0005-0007 LT), before discussing the more complex and less clear cases shown in Figure 4 (28 Dec, 0112-0115 LT) and then Figure 5 (28 Dec, 0112-0115 LT)?

Authors' response:

Taking the reviewer's suggestion, all the speculative statements have been dropped, the remaining part becomes the following form.

"To further clarify the microphysical process of precipitating hydrometeors, two sets of representative lidar profiles (X, δ_v and q_v) for the period that precipitation reached the surface (in Fig.2) are plotted in Figs. 4 and 5. Figure 4 gives three 1-min X and δ_v profiles from 0112 to 0114 LT on 28 December 2017 and a one-hour-averaged q_v profile centered at 0113 LT on the same day. The lidar dark band appeared at a 2.88-km altitude at approximately 0113 LT, while the local δ_v minimum (<0.04, far less than the δ_v-based discrimination threshold value of spherical particles when the lidar backscatter ratio $R \geq 5$) was located at a 2.76-km altitude. These altitudes represent a typical lidar signature of the snowflake-to-raindrop transition for a variety of stratiform precipitation events." (please see P9, lines 248-253)

The authors sincerely thank the reviewer for his/her friendly suggestion. Since the focus of this study is the precipitation process that reaches the surface, the discussion of the lidar observations with Figure 6 (the virga during the short period between two reaching-surface precipitations) is to simply help us understand the complete vertical structure of precipitating hydrometeors and their apparent source cloud, because it is undetectable due to strong optical attenuation when the precipitation reached the surface. Please allow us to follow this expression logic.

Comments:

P9, l269-277: Please keep in mind: The decrease of VDR355 below the VDR355 maximum at 600 m height can also be the result of the increasing influence of non-depolarizing boundary-layer aerosol particles. The backscatter coefficient (in your case the range-corrected signal) strongly increases with decreasing height, probably caused by strong aerosol pollution.

Authors' response:

The magnitude of the lidar-measured volume depolarization ratio allows us to discriminate whether the dominant lidar backscattering is attributed to spherical or nonspherical particles in a given backscatter volume. Considering that the complete-overlap altitude of our polarization lidar is reliably less than 400 m, we here examine in the altitude range of ~400–600 m whether the decrease of δ_v (VDR355) below its maximum at ~600-m altitude would be a result of increasing influence of non-depolarizing boundary-layer aerosol particles or not. As seen in Figure 10 in the revised manuscript, the value of the volume depolarization ratio δ_v is 0.31 (a mean of three profiles) at ~600-m altitude and decreases to ~0.20 at 400-m altitude. Obviously, the dominant lidar backscattering (yielding δ_v = ~0.20) at the altitude of 400 m should be attributed to nonspherical rain drops. Such a significant δ_v decrement ($\Delta\delta_v$=0.11) in the altitude range of 200 m should be explained as the depolarization variation of the nonspherical rain drops themselves rather than the increasing impact of non-depolarizing boundary-layer aerosol particles. In addition, noticing that the δ_v maxima (~0.27–0.35) at ~0.6-km altitude shown in Figure 10 were corresponding well to the high rainfall rate of 3.2 mm h^{-1} (rain gauge record on the ground), it is difficult to say that the non-depolarizing boundary aerosol particles (at a rainy night) could strongly change the depolarization of a large-raindrop-dominant backscatter volume.

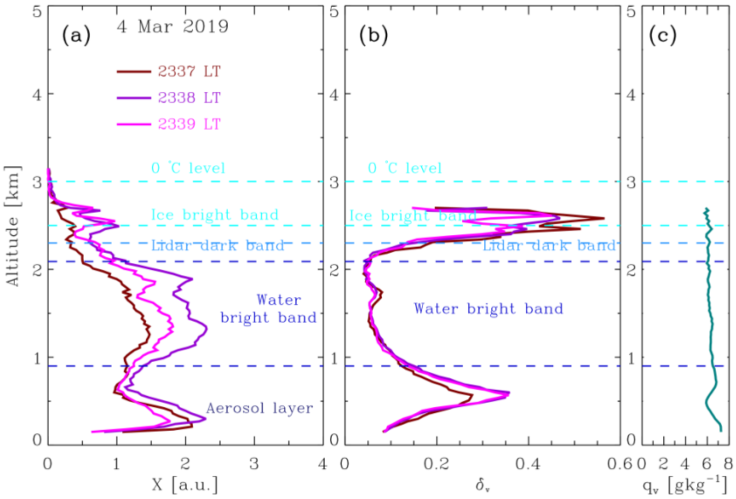

Figure 10: Three 1-min lidar X and δ_v profiles covering the period from 2337 to 2339 LT on 4 March 2019 and a one-hour-averaged lidar q_v profilecentered at 2338 LT on the same day, exhibiting the vertical structure of the X and δ_v precipitation streaks as well as the water vapor mixing ratio when the surface precipitation rate was highest (3.2 mm h^{-1}) during the studied moderate warm-front precipitation event.

Comments:

P10, l285: One should clearly and more often emphasize that the radiosonde temperatures were most probably measured in virga-free air. This is needed to avoid the impression that temperatures were up to 5°C in the virga with ice crystals. The temperatures in the virga were most probably always close to 0°C.

Authors' response:

Taking the reviewer's suggestion, we have added a statement "However, it should be mentioned here that the radiosonde launching site was ~23.4 km away from our lidar site." (please see P11, l313-314)

Comments:

P10, l295-315: As mentioned, VDR355 is a function of the particle-to-molecular backscatter, and thus a function of the particle backscatter coefficient BSC355. With increasing BSC355, the difference between VDR355 and PDR355 decreases. In lines 308-310, you mention the inverse relationship between backscatter and VDR355. Exactly that prevents you to make clear statements about the presence and number concentrations of droplets and ice crystals. The better parameter would be PDR355. To obtain PDR355 from VDR355 you need, however, to calculate the height profile of BSC355 first. BSC355 and PDR355 would allow a much better discussion, instead of using the basic and just qualitative lidar quantities, VDR355 and range-corrected signals. This is not just state-of-the-art.

Authors' response:

The authors sincerely appreciate the reviewer for encouraging us to utilize the state-of-the-art parameters δ_p (PDR355) and β_p(BSC355) in describing the lidar-observed results. Here please allow us to explain why the δ_v (VDR355) and X (attenuated backscatter355) have been employed in the current cloud/precipitation study rather than δ_p (PDR355) and β_p (BSC355).

The determination of the particle backscatter coefficient β_p needs to introduce additional assumptions. The data retrieval of the elastic lidar return suffers from the fact that the two unknowns (the particle backscatter coefficient β_p and particle extinction coefficient α_p) must be determined from only one measured quantity (one lidar equation). Thus, an additional assumption is introduced to settle this problem. *Fernald* developed an algorithm to derive the two unknowns by assuming that the ratio of particle extinction coefficient to backscatter coefficient (lidar ratio) was a given constant value. This lidar ratio assumption is usually not true in the real atmosphere. A vibration-rotational Raman lidar that detects both elastically backscattered signal from air molecules and aerosols and Raman backscattered signal by N_2 (or O_2) molecules can yield two lidar equations. The two equations however include three unknown aerosol optical parameters, i.e., particle extinction coefficients at the transmitted wavelength and Raman-shifted wavelength as well as particle backscatter coefficient at the transmitted wavelength. Then an assumed wavelength dependence (i.e., the *Ångström* relationship) on the particle extinction coefficient must be introduced to obtain the solutions for the aerosol optical properties at the transmitted wavelength. The additional assumptions apparently result in quantitative uncertainties in estimated particle backscattter and extinction coefficients. Furthermore, for the lidar measurements during precipitation and its precursor cloud, it is in general impossible to obtain a "reference height" with particle backscatter coefficient β_p(BSC355) being negligible compared to the molecular backscatter value β_m. Then the numerical solution of the particle backscatter coefficient β_p is not attainable by the conventional Fernald retrieval method. The uncertainty in β_p(BSC355) would lead to an uncertainty of δ_p (PDR355) value derived from the δ_p expression Equation (1) (Cairo et al., AO, 1999).

The δ_v (VDR355) and X are basic lidar-measured quantities. According to the discussion above, for precipitation-related cloud/virga in this study (lidar backscatter ratio R >7), the quasilinear functional relationship between δ_p (PDR355) and δ_v (VDR355) enables us to discriminate water droplets and ice crystals in a given backscatter volume of cloud/virga by using δ_v (VDR355) whose magnitude is slightly smaller than that of the corresponding δ_p value.

The inverse relationship between X and δ_v occurred at the ice-bright-band altitudes where R >7. Inputting parameters R=7 and δ_m=0.004 into Equation (1), we obtain the moderate δ_p minima (~0.09–0.12) at ~3.0-km altitude that correspond to the moderate δ_v minima (~0.08–0.10). Accordingly, the markedly enhanced δ_v values (~0.17–0.34) are equivalent to the markedly enhanced δ_p values (~0.20–0.42). Therefore, the statements about the presence of high-concentration partially melted large particles at ~3.0-km altitude, and ice crystals and large snowflakes at higher altitudes (3.06–3.21 km) would be correct still.

Comments:

P11, l315-335: This is the best part of the entire discussion! Nevertheless, the detection of the liquid-water cloud deck does not mean that the ice crystals formed in this layer. We do not have any information about potential cloud seeding effects …. from above so that ice nucleation may have taken place at -25°C. Nobody knows.

Authors' response:

The authors greatly appreciate the reviewer for his/her kind encouragement. We have noticed that the water vapor mixing ratio q_v usually showed an overall decrease with increasing altitude during stratiform precipitations (e.g., Figure 3c and Figure 8c). This suggests that the liquid-water cloud deck immediately above precipitating hydrometeors might be a main source cloud of precipitation. At higher altitudes above the liquid-water cloud deck, less water vapor (supply) would prevent the formation of high-concentration liquid-droplet cloud.

Comments:

P11, l329-330: Again, do not forget that VDR355 changes with BSC355 (or the particle-to-molecular backscatter). VDR355 is thus influenced by ice crystals, droplets, and Rayleigh molecules. There is a mixture of information from molecules (1% depolarization) and particle (droplets 0-5%, crystals around 40%). And the lower BSC355, the lower the VDR355. In the case of PDR355, you would be able to make much more clear statements about the presence of droplets and crystals, because the Rayleigh impact is removed.

Authors' response:

The δ_v (VDR355) is a basic lidar-measured quantity. According to the discussion above, for precipitation-related cloud/virga in this study (lidar backscatter ratio R >7), the quasilinear functional relationship between δ_p (PDR355) and δ_v (VDR355) enables us to discriminate water droplets and ice crystals in a given backscatter volume of cloud/virga by using δ_v (VDR355) whose magnitude is slightly smaller than that of the corresponding δ_p value.

Taking the reviewer's comment into account, the earlier statements (l329-330) have changed to

"According to the expressions on the right-hand sides of Inequalities (1) and (2), the δ_v-based discrimination threshold values were respectively 0.09 for spherical particles and 0.17 for nonspherical particles when the lidar backscatter ratio R had a value of 7 (the minimum of the R value range) on the upper part of the precipitation-related virga (Lampert et al., 2010; Cheng and Yi, 2020). Thus, the δ_v magnitude of the falling virga increased from the liquid-water values of ~0.02–0.07 (< 0.09) at an altitude of 4.38 km to the ice/snow values of ~0.21–0.33 (> 0.17) at an altitude of 4.02 km." (please see P12, lines 354-359 in the revised manuscript)

Comments:

P11, l346: Again, to my opinion, the falling hydrometeors in the first 100-200m of *their descent are ice crystals. Variations in VDR355 are probably caused by the variations in the particle-to-molecule backscatter ratio.*

Authors' response:

According to our discussions above, for R=7 which corresponds to the main part of the precipitation-related virga (Lampert et al., 2010; Cheng and Yi, 2020), the discrimination criterion of water droplets δ_p < 0.1 (in terms of the particle depolarization ratio δ_p) is equivalent to δ_v <0.09 (in terms of the volume depolarization ratio δ_v), while the discrimination criterion of ice crystals δ_p > 0.2 is equivalent to δ_v > 0.17. Taking the reviewer's comment into account, the earlier sentence (l346) has changed to "The depolarization ratio magnitude of falling hydrometeors increased from the liquid-water values (δ_v< 0.09) to the ice/snow values (δ_v > 0.20) during the first 100–200 m of their descent" (please see P12-13, lines 374-376 in the revised manuscript). It states simply the lidar-observed results.

As mentioned above, the earlier in-situ and lidar observations have indicated that some virgae falling out of the supercooled liquid stratiform clouds did contain detectable liquid water drops (Rangno and Hobbs, JGR, 2001; Ansmann et al., 2008, please see Fig. 8 and paragraph 52; Yi et al, AR, 2021).

Comments:

P12, l350: The Hallet-Mossop effect (secondary ice formation, SIF) causes a rather huge increase (orders of magnitude) in ice crystal number concentration at temperatures between -5 and -8°C. To my understanding, SIF is very efficient in the mixed-phase clouds (in the main cloud body with dense populations of crystals and droplets). So, my question is: Is SIF also very strong in (ice-dominating) virga? Can you provide references that SIF occurs in virga as well?

Authors' response:

The authors thank the reviewer for alerting us to the Hallett-Mossop process of ice splinter production during riming. Because the reaching-surface rainfall was closely related to the formation of large particles in falling hydrometeors (from the mid-level stratiform cloud), the riming was assumed here as a production mechanism (similar to aggregation) of large particles. Our current lidar-observations cannot answer if the secondary ice formation was very strong in ice-dominating virga. We have raked some literatures, but the references about the secondary ice formation in virga are unavailable.

Comments:

P12, l350-373: Again, it would be helpful to have PDR355 instead of VDR355 in the discussion.

Authors' response:

In light of the previous numerical and analytical discussions to the δ_p (PDR355) expression (Cairo et al., 1999), for precipitation-related cloud/virga in this study (lidar backscatter ratio R >7), the functional dependence of δ_p (PDR355) upon δ_v (VDR355) is quasilinear with a zero offset and an apparent slope slightly larger than 1 (the nonlinear term belongs to high-order small quantity). This favorable relationship enables us to discriminate spherical water drops/droplets and ice crystals in a given backscatter volume of cloud/virga by using δ_v (VDR355) whose magnitude is slightly smaller than that of the corresponding δ_p value. Specifically, when R=7, the discrimination criterion of spherical water drops/droplets $\delta_p < 0.1$ (in terms of the particle depolarization ratio δ_p) is equivalent to $\delta_v < 0.09$ (in terms of the volume depolarization ratio δ_v), while the discrimination criterion of ice crystals $\delta_p > 0.2$ is equivalent to $\delta_v > 0.17$. Such small differences in the discrimination threshold values together with the quasilinear functional relationship between δ_p and δ_v enable us to discriminate spherical water drops/droplets and nonspherical ice crystals in a given backscatter volume of cloud/virga by using δ_v (VDR355). Even if the discrimination criteria are given strictly in terms of the commonly-used values of particle depolarization ratio δ_p ($\delta_p < 0.1$ or its equivalent $\delta_v < 0.09$ for spherical water drops/droplets, and $\delta_p > 0.2$ or its equivalent $\delta_v > 0.17$ for nonspherical ice crystals), all the results expressed in this paper are still valid.

In practice, as shown by this manuscript, the lidar-observed volume depolarization ratio δ_v has correctly demonstrated the vertical structure of precipitating hydrometeors from mid-level stratiform clouds (e.g., an ice/snow part above and a liquid-water part below as well as a clear-cut melting layer, please see Figures 2b and 7b), indicating that the volume depolarization ratio δ_v can also do a good job for cloud/virga. This is consistent with the earlier literatures (Wang and Sassen, 2001; Intrieri et al., 2002; Shupe, 2007; Ansmann et al., 2009; Lampert et al., 2010).

Taking the reviewer's comment into account, the "($\delta_v \leq 0.04$)" in this pat (P12, l350-373) has changed to "($\delta_v \leq 0.04$, far less than the δ_v-based discrimination threshold value of spherical particles when $R \geq 5$)" (please see P13, lines 381-382 in the revised manuscript).

Comments:

P12, l375: Figure 7 shows again, that you can observe and describe virga properties. But there is no way to say anything about the ice nucleation processes higher up. The cloud deck in which ice crystals were initially nucleated remains undetected.

Authors' response:

All the statements related to Figure 7 (the second example) have been checked carefully. We have not found any words about the ice nucleation processes higher up.

Comments:

P12, l380-395: Again, the discussion is based on VDR355…. Low and high values are mainly controlled by the particle-to-molecule backscatter ratio (or BSC355), and only if particle backscattering is very high, VDR355 comes close to the particle-related PDR355.

Authors' response:

In order to clarify whether the low δ_v (VDR355) values (28 Dec 2017) correspond to the low δ_p (PDR355) values, and the high δ_v (VDR355) values (4 Mar 2019) correspond to the high δ_p (PDR355) values when the lidar backscatter ratio R varies in the range of all possible R values, we start with the strict δ_p (PDR355) expression (Equation (1)) (Cairo et al., 1999)

$$\delta_p(\mathrm{z}) = \frac{(1+\delta_m)\delta_v(\mathrm{z})R(z)-(1+\delta_v(\mathrm{z}))\delta_m}{(1+\delta_m)R(z)-(1+\delta_v(\mathrm{z}))}, \quad (1)$$

where the δ_m value is ~0.004 for our 0.3-nm bandwidth polarization lidar (355 nm).

On 28 Dec 2017, the lidar-measured δ_v had a mean value of ~0.3 on the ice bright band (please see Figs. 4b&5b in the revised manuscript). The corresponding mean (δ_v) value was ~0.4 on 4 Mar 2019 (please see Figs. 9b&10b in the revised manuscript). Inserting the two δ_v values (as parameters) into Equation (1), the δ_p (PDR355) is calculated as a function of R (plotted in Figure R7). As seen in Figure R7, all the δ_p values on the curve for δ_v =0.4 are larger than those on the curve for δ_v =0.3 in the entire range of possible R values (5-100, the R values should be larger than 7 for the precipitation-related virga). Figure R7 indicates that the δ_p (PDR355) magnitude is mainly controlled by the δ_v (VDR355) magnitude (low and high values), and has a very weak dependence on lidar backscatter ratio R. In other words, on the ice bright band, the large δ_v values corresponds to large δ_p values (on 4 Mar 2019), while the small δ_v values to small δ_p values (on 28 Dec 2017).

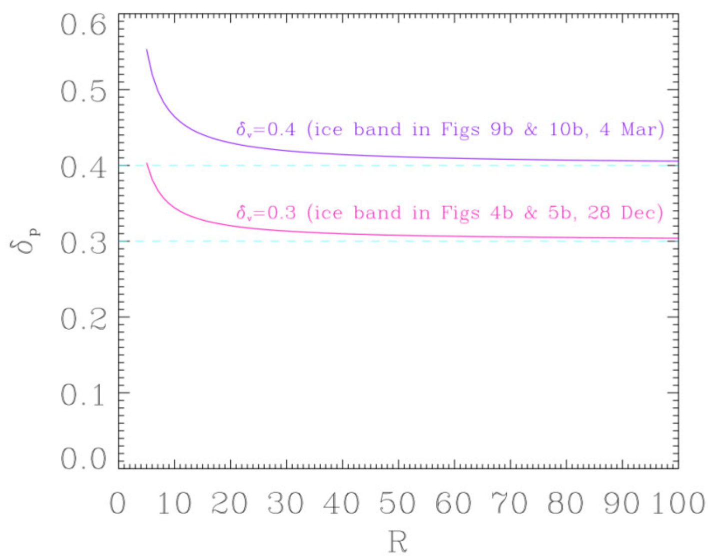

Figure R7. The particle depolarization ratio δ_p as a function of lidar backscatter ratio R for the lidar-measured volume depolarization ratio δ_v (VDR355) values on the two different days (28 Dec 2017 and 4 Mar 2019). The δ_v =~0.3 and δ_v =~0.4 are the average values on the ice bright band respectively from Figs.4b & 5b (28 Dec 2017) and Figs. 9b &10b (4 Mar 2019). Note that all the δ_p values on the curve for δ_v =0.4 are obviously larger than those on the curve for δ_v =0.3 in the entire range of possible R values (5-100).

On 28 Dec 2017, the lidar-measured δ_v had a mean value of ~0.15 at ~0.6-km altitude (please see Figs. 4b&5b in the revised manuscript). The corresponding mean (δ_v) value was ~0.28 on 4 Mar 2019 (please see Figs. 9b&10b in the revised manuscript). Similarly, inserting the two δ_v values into Equation (1), the δ_p (PDR355) is calculated as a function of *R* (plotted in Figure R8). As seen in Figure R8, all the δ_p values on the curve for δ_v =0.28 are obviously larger than those on the curve for δ_v =0.15 in the entire range of possible *R* values (3-100).

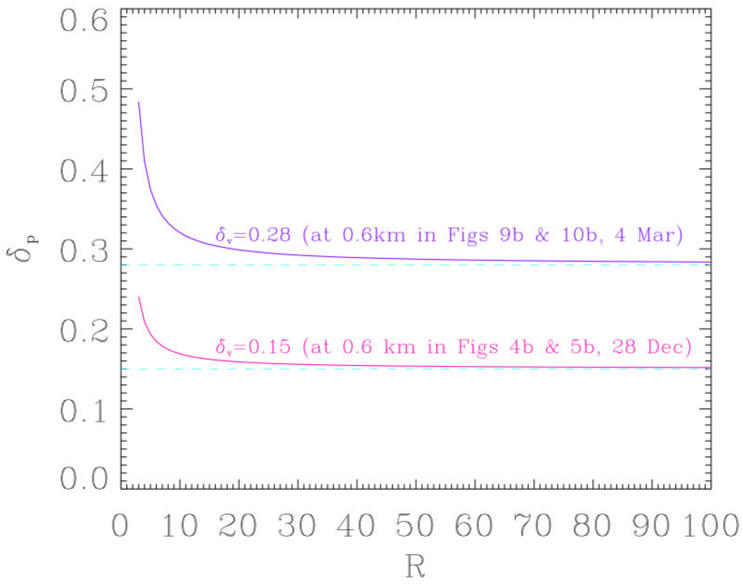

Figure R8. The δ_p (PDR355) as a function of lidar backscatter ratio *R* for the lidar-measured volume depolarization ratio δ_v (VDR355) values on the two different days (28 Dec 2017 and 4 Mar 2019). The δ_v =~0.15 and δ_v =~0.28 are the average values at ~0.6-km altitude respectively from Figs.4b & 5b (28 Dec 2017) and Figs. 9b &10b (4 Mar 2019). Note that all the δ_p values on the curve for δ_v =0.28 are obviously larger than those on the curve for δ_v =0.15 in the entire range of possible *R* values (3-100).

Based on the numerical analysis above, all the discussions (P12, l380-395) based on the lidar-measured volume depolarization ratio δ_v (VDR355) are valid.

Comments:
The same statements about BSC355 vs VDR355 relationship hold for the final section 3.2.2.

Authors' response:

The validity of the δ_v (VDR355)-based discussions at altitudes of the ice bright band and δ_v maxima around 0.6 km in the section 3.2.2 has been confirmed by the numerical analysis above. As a supplement, now we examine for the water bright band, whether the low δ_v (VDR355) values correspond to the low δ_p (PDR355) values, and the high δ_v (VDR355) values correspond to the high δ_p (PDR355) values when the lidar backscatter ratio *R* varies in the range of all possible *R* values. As seen from Figure 10b in the revised manuscript, "in the height range of the water bright band, the depolarization ratio (δ_v) increased from ~0.04–0.06 at an altitude of approximately 2.09 km to ~0.12–0.15 at an altitude of 0.9 km, indicating that more large raindrops formed via collision-coalescence processes therein" (please see P15-16, l471-474 in the revised manuscript). Similarly, inserting the two δ_v mean values (0.05 and 0.135) into Equation (1), the δ_p (PDR355) is calculated as a function of R (plotted in Figure R9). As seen in Figure R9, all the δ_p values on the curve for δ_v =0.135 are obviously larger than those on the curve for δ_v =0.05 in the entire range of possible R values (3-100). Hence all the discussions based on the lidar-measured volume depolarization ratio δ_v (VDR355) are valid in the section 3.2.2.

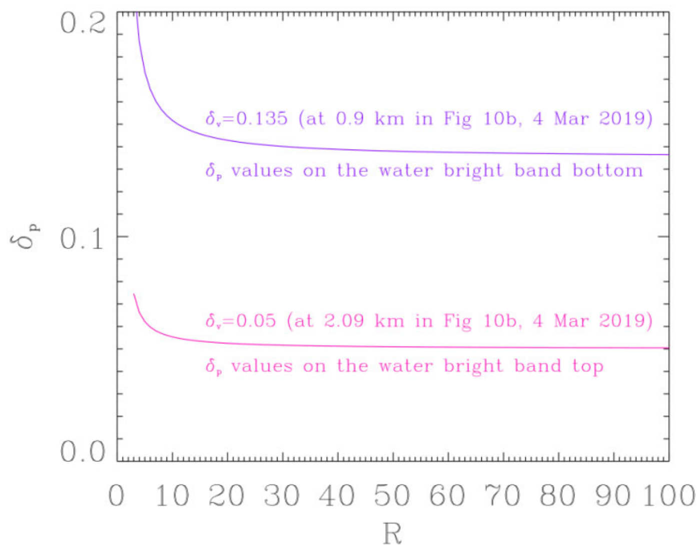

Figure R9. The δ_p (PDR355) as a function of lidar backscatter ratio R for the lidar-measured volume depolarization ratio δ_v (VDR355) values at two different altitudes (Fig. 10b, 4 Mar 2019). The δ_v =0.05 and δ_v =0.135 are the average values at 2.09-km and 0.9-km altitudes respectively as shown in Fig. 10b (4 Mar 2019). Note that all the δ_p values on the curve for δ_v =0.135 (at the water bright band bottom) are obviously larger than those on the curve for δ_v =0.05 (at the water bright band top) in the entire range of possible R values (3-100).

Comments:

P15, l470-475: You did not clearly observe any cloud layer in which ice nucleated. The focus in this manuscript is on the discussion on virga, and nothing else.

Authors' response:

The statements in this pat (P15, l470-475) have briefly described the lidar-observed warm-front-related precursor clouds and associated meteorological conditions. There are no words about the cloud layer in which ice nucleated.

Comments:

P16, l485: You do not have any observation that clearly indicates that you measured a mixture of droplets and ice crystals here….. VDR355 does not allow such conclusions. PDR355 would allow that. To my opinion, the virga purely consist of ice crystals.

Authors' response:

In order to clarify whether the depolarization ratio magnitude of falling hydrometeors increased from the liquid-water values to the ice/snow values during the first 100–200 m of their descent (please see Fig.6b, 28 Dec 2017), we start with the strict δ_p (PDR355) expression (Equation (1)) (Cairo et al., 1999)

$$\delta_p(z) = \frac{(1+\delta_m)\delta_v(z)R(z)-(1+\delta_v(z))\delta_m}{(1+\delta_m)R(z)-(1+\delta_v(z))}, \quad (1)$$

where the δ_m value is ~0.004 for our 0.3-nm bandwidth polarization lidar (355 nm).

On 28 Dec 2017, the lidar-measured δ_v had the mean values of ~0.059 at 4.35-km altitude and ~0.037 at 4.38 km (on the ice virga top, please see Fig.6b in the revised manuscript). Inserting the two δ_v values (as parameters) into Equation (1), the δ_p (PDR355) is calculated as a function of *R* (plotted in Figure R3). As seen in Figure R3, all the δ_p values on the curves for δ_v =0.059 and δ_v =0.037 are smaller than 0.1 in the entire range of possible *R* values (7-100, the R values should be larger than 7 for the precipitation-related virga). The maximum δ_p values on the curves are respectively 0.069 at 4.35-km altitude and 0.042 at 4.38 km (corresponding to *R*=7), indicating that the dominant lidar backscattering should be attributed to spherical water drops/droplets at these altitudes.

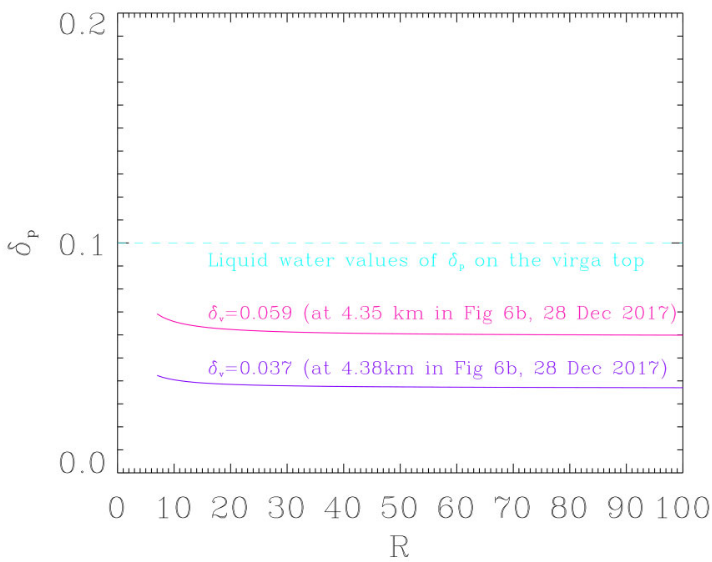

Figure R3. The δ_p (PDR355) as a function of lidar backscatter ratio *R* for the lidar-measured volume depolarization ratio δ_v (VDR355) values at two different altitudes (Fig. 6b, 28 Dec 2017). The δ_v =0.059 and δ_v =0.037 are the average values at 4.35-km and 4.38-km altitudes respectively as shown in Fig. 6b (28 Dec 2017). Note that all the δ_p values on the curves for δ_v =0.059 and δ_v =0.037 (at the ice virga top) are clearly less than 0.1 in the entire range of possible *R* values (7-100).

On the same day (28 Dec 2017), the lidar-measured δ_v had the mean values of ~0.220 at 4.17-km altitude and ~0.259 at 4.02 km (at altitudes ~180–330 m below the

the ice virga top, please see Fig.6b in the revised manuscript). Inserting the two δ_v values (as parameters) into Equation (1), the δ_p (PDR355) is calculated as a function of R (plotted in Figure R4). As seen in Figure R4, all the δ_p values on the curves for δ_v =0.220 and δ_v =0.259 are larger than 0.2 in the entire range of possible R values (7-100, the R values should be larger than 7 for the precipitation-related virga). The minimum δ_p values on the curves are respectively 0.223 at 4.17-km altitude and 0.262 at 4.02 km (corresponding to R=100), indicating that the dominant lidar backscattering should be attributed to nonspherical ice crystals at these altitudes.

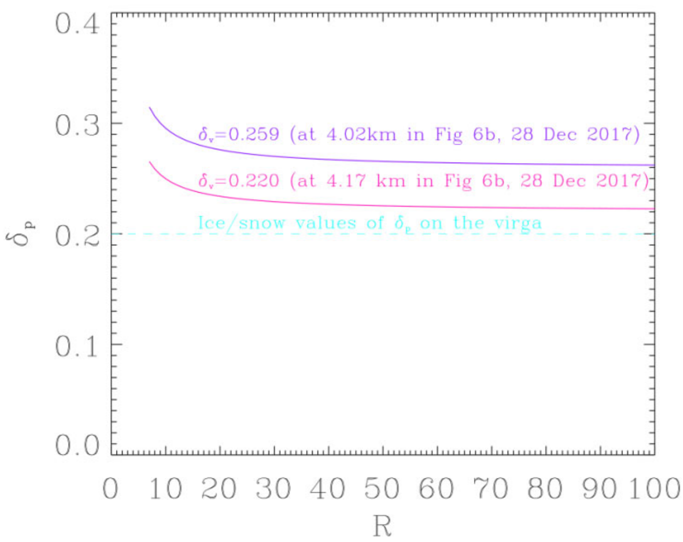

Figure R4. The δ_p (PDR355) as a function of lidar backscatter ratio R for the lidar-measured volume depolarization ratio δ_v (VDR355) values at two different altitudes (Fig. 6b, 28 Dec 2017). The δ_v =0.220 and δ_v =0.259 are the average values at 4.17-km and 4.02-km altitudes respectively as shown in Fig. 6b (28 Dec 2017). Note that all the δ_p values on the curves for δ_v =0.220 and δ_v =0.259 (at altitudes ~180–330 m below the ice virga top) are clearly larger than 0.2 in the entire range of possible R values (7-100).

Figure R3 and R4 indicate that the δ_p (PDR355) magnitude is mainly controlled by the δ_v (VDR355) magnitude (low and high values), and has a very weak dependence on lidar backscatter ratio R. Hence the conclusion "The depolarization ratio magnitude of falling hydrometeors increased from the liquid-water values (δ_v < 0.09) to the ice/snow values (δ_v> 0.20) during the first 100–200 m of their descent" (P17, l514-516) should be allowable.

With respect to whether all virgae above the height of the 0°C-level consist of ice crystals or not, we have noticed some interesting observational results shown in the earlier literatures. The airborne in-situ measurements show that there sometimes existed detectable liquid water content (LWC) at altitudes of ice virgae (Carey et al., JAMC, 2008, please Figs.1b, 1e-1g). In addition, the drizzle-sized water drop virgae (no ice) were observed beneath thin liquid cloud layers with cloud top temperatures of 0° to –4°C (Rangno and Hobbs, JGR, 2001; Yi et al, AR, 2021), indicating that precipitation-sized particles can form through turbulence (or weak updraft)-induced collision-coalescence process in the thin liquid cloud layers. The similar mechanism should work in an earlier observational example that the virga mainly consisted of drops rather than ice for a moderately supercooled stratiform cloud at temperatures as low as −14°C (Ansmann et al., 2008, please see Fig. 8 and paragraph 52).